폭발챔버에서 전파하는 화염의 국부 거동

박달재 · 이영순†
서울과학기술대학교 공과대학 안전공학과
(2010. 12. 13. 접수 / 2011. 3. 11. 채택)

Local Behaviour of Propagating Flames in an Explosion Chamber

Dal-Jae Park · Young-Soon Lee†
Department of Safety Engineering, Seoul National University of Science and Technology
(Received December 13, 2010 / Accepted March 11, 2011)

Abstract : Experimental studies were carried out in an explosion chamber to investigate the influences of multiple cylinder obstacles on local flame propagation. The chamber dimension is 235 mm in height with a 1,000×950 mm^2 rectangular cross section and a large vent area of 1,000×320 mm^2. Multiple cylinder bars with obstruction ratio of 30% were used. In order to examine the interaction between the propagating flames and the obstacles, temporally resolved flame front images were recorded by a high speed video camera. The propagation behaviour of local flame fronts around the left obstacle was analyzed in terms of two different methods such as the incremental burnt area divided by the flame front length and the average of the local propagation velocity determined at each point along the flame front. It was found that two methods give good consistency.

초 록 : 다중 장애물을 가지는 폭발챔버에서 전파하는 화염과 국부 장애물의 상관관계를 조사하기 위하여 실험적 연구를 수행하였다. 폭발챔버 높이 235 mm, 단면적 1,000×950 mm^2, 벤트면적 1,000×320 mm^2를 가지는 폭발챔버를 제작하였으며, 30% blockage ratio를 가지는 장애물을 챔버내에 설치하였다. 전파하는 화염과 장애물의 상관관계를 조사하기 위해 고속카메라를 사용하였다. 고속카메라로 얻어진 화염 이미지로부터 장애물 주위의 국부 화염전파 거동은 2가지 다른 방법, 즉 전파하는 화염전면(flame front)의 각 pixel point에서 산정된 평균 화염전파속도와 연소면적 증가(incremental burnt area)/화염전면 길이(flame front length) 관점에서 분석하였다. 분석결과, 2가지 방법으로 얻은 결과는 거의 일치하는 경향을 나타났으며, 전파하는 화염이 장애물의 전면과 상호 작용할 때 화염속도는 급격히 증가하다가 장애물의 후단면에서 약간 감소하고, 화염이 장애물 후단에서 재결합될 때 다시 급격히 증가하였다.
Key Words : averaged flame velocity, incremental burnt area, flame front length, obstacle

1. Introduction

Gas explosions have a great implication on the safety in terms of potential loss of life, destruction of property and buildings, business interruption risks, etc. In particular, explosions occurring in confined and partially-confined regions are of special interests due to the domino effects and more serious consequences[1]. The interaction between the flame and the local obstruction caused by the existence of equipments like pipe-work and vessels results in local flame acceleration of the propagating flame front[2]. The influences of such local blockage on explosion process were performed by many investigators[3-6].

The studies based on large length to diameter (L/D) ratio reported that there is a strong interaction between the turbulence level formed in the wake of the obstacle and the resulting peak pressure. However, the more detailed data of local flame velocities between the propagating flame front and obstacles have not been reported.

The main objectives of current work are at providing the experimental data of the local flame propagation velocities around the obstacle and investigating the underlying mechanisms of local flame/obstacle interaction in a partially opened enclosure with a

† To whom correspondence should be addressed.
lysoon@snut.ac.kr

small L/D ratio and a large vent area.

2. Experimental

The explosion chamber, apparatus and experimental methods used in this work are the same with the experiments described in previous work[1].

Fig. 1 displays a schematic diagram of the experimental set-up consisting of an explosion chamber, 235 mm in height, 1,000 × 950 mm^2 in cross-sectional area and with a large top-venting area of 1,000 × 320 mm^2. This gives a total volume of 223 liters of explosive mixture and a $A_v/V^{2/3}$ ratio of 0.8695. The rig was made of 20 mm thick transparent chemiglass. Flammable gas(99.9% CH_4 by vol.) entered the chamber through the valve positioned in the bottom of the side wall of the chamber. The fuel volume flow rates were monitored by a calibrated gas flow control system(TEI, Model GFC 521).

Before gas filling, the large rectangular vent was covered with thin plastic film(house hold plastic wrap). The film was sealed on a layer of blue tak lined around the vent. Air within the chamber during the filling sequence was continuously withdrawn via the open sample ports placed at three different locations. The fuel/air mixture was circulated through the explosion chamber using a recirculation pump to ensure a completely homogeneous mixture. The fuel concentration was monitored by an infrared gas analyzer(GDA, Model LMSx) with an accuracy of ±0.3%. The calibration of the apparatus was periodically checked by injecting calibration gases of known composition into the measurement system.

The flammable mixture in the chamber was ignited by a 15.5 KV electric spark positioned at the centre of the bottom wall. The flame images were recorded using a high speed video camera(KODAK Motion Recorder Analyzer, SR-ULTRA-C) operating at the rate of 500 frame/s, providing a temporal resolution of 2 ms.

As shown in Fig. 1, multiple cylindrical obstacles with obstruction ratio of 30% were installed inside the chamber and centred 117.5 mm from the bottom of the chamber. The estimation of obstruction ratio is an area percentage defined as the largest cross-sectional area blocked by positioning the obstruction in the explosion chamber divided by the cross-sectional area of the explosion chamber which is 1,000 × 950 mm^2 [5]. The methane concentration in air during the measurements was 10 ± 0.2%.

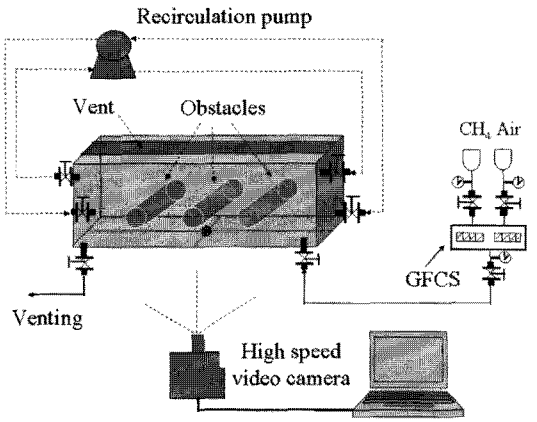

Fig. 1. Schematic diagram of the experimental set-up.

The procedures to examine the local flame-front characteristics are the same with the previous study[1]. In this study, its are divided into the following three steps:

(1) Identification of the region of interest

As displayed in Fig. 2(a), the local region of interest selected here was around the left obstacle. The sub-region area was 100 × 100 $pixels^2$ with the centre of the obstacle coincide with that of the region of interest.

(2) Image processing

Fig. 2(b) displays one example of image processing applied in the area of interest to the original flame image obtained at 120 ms after ignition. Image analysis was done by using the Optical Multi-channel Analyser tool for all the images obtained form the high speed video camera. A 5 by 5 smoothing filter is applied initially before the image is made binary. The red colour shows the burnt area and the block one is the unburnt area including the circular obstacle. A sequence of images can be processed to analyze the local flame propagation around the left obstacle and the flame-front boundary is determined for each individual image.

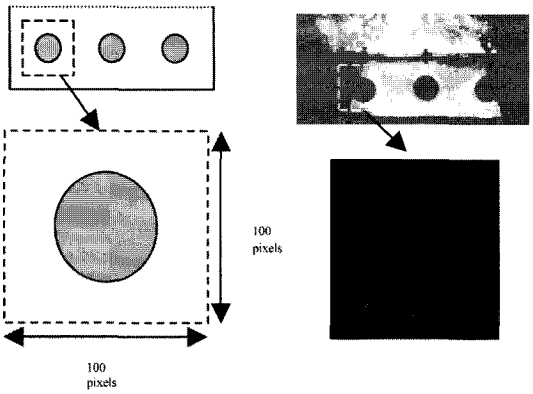

Fig. 2. (a) Selection of a local region of interest; (b) Example of image processing applied to the original flame image in the region of interest.

(3) Flame front tracking

The flame-front contour coordinates of each image can be extracted by using an in-house FORTRAN code. All points along the contour are separated by 1 pixel, and one pixel here is 2 mm. With the coordinates of the contour, the flame front length and local flame front displacement in the normal direction between two consecutive images were calculated. Local flame propagation velocity was determined along the flame front by dividing the distance along the normal line at each point by the time between images.

3. Results and Discussion

Fig. 3 displays a sequence of temporally resolved flame-front images in the area of interest. The time shown below each image shows the elapsed time after ignition and subsequent flame images are at 2 ms intervals. The propagating flame front moves laterally toward the left obstacle and reaches the right side of the obstacle at about 96 ms after ignition. After impinging on the obstacle, the segment of flame front above the obstacle was found to propagate slower than the lower segment of the flame front.

With increasing time after impingement, the flame starts to roll up around the obstacle, and the flame decelerates. This is seen in Fig. 4(a) where the temporal increase of the burnt area, A, slows down slightly with time. After flame deceleration, the flame burns into the wake and the propagation flame front

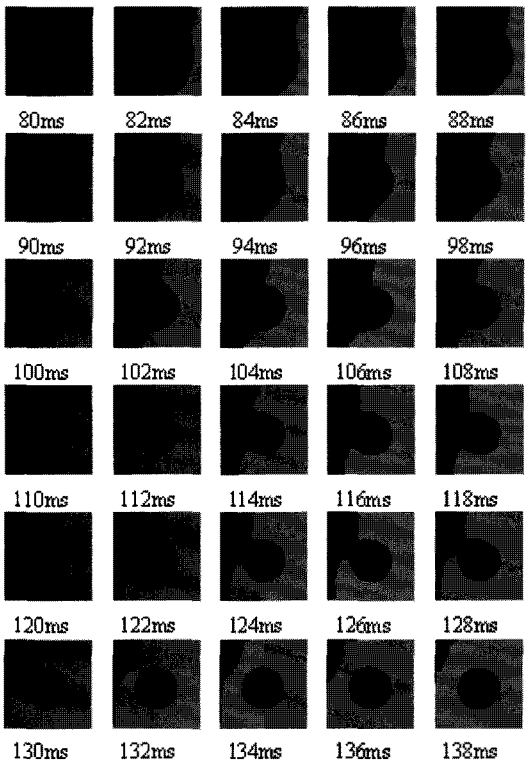

Fig. 3. A temporal sequence of flame images in the area of interest displaying flame propagation around the left obstacle.

reconnects, the flame accelerates again. The flame surface area is greatly increased at this stage and hence the burning rate. Flame reconnection behind the obstacle occurred at about 134 ms after ignition.

Fig. 4(b) displays a comparison of the average of the local flame propagation velocity, S_{av}, derived via two different methods from 80 ms to 140 ms after ignition. The first method is from the incremental burnt area, $\triangle A$, divided by the flame front length, L; the second one is from the average of the local flame propagation velocity determined at each point along the flame front. In the first method, the flame front length touched with the obstacle is not included at the calculation of the flame front length. The results from both methods showed good consistency, as expected.

The local flame propagation velocity remains fairly constant at approximately 2 m/s before the flame impinges onto the obstacle. The much higher value of the flame propagation velocity than the laminar burn-

ing velocity is due to the expansion effect as actually it is the burnt gas velocity that is measured here.

Much higher burning velocity is found at the early stage of flame impingement onto the obstacle. Despite some fluctuations, the general trend of the local propagation velocity is decreasing when the flame passes over the obstacle from 96 ms to 126 ms after the ignition. Only as the flame has passed over the obstacle, the local burning velocity increased again most likely due to turbulent generated behind the obstacle.

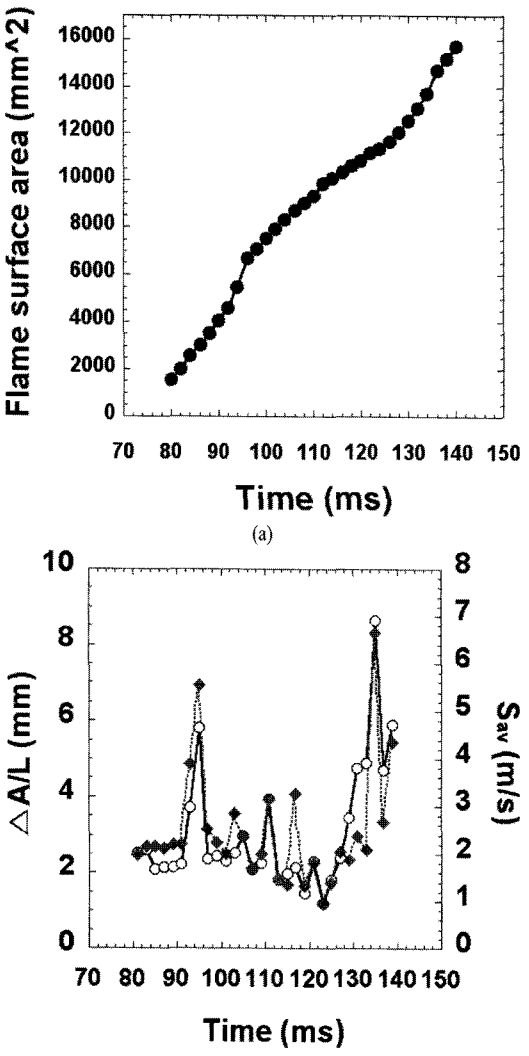

Fig. 4. (a) The flame area of local burnt area with time and (b) The incremental burnt area (△A) divided by the flame front length (L) and the average of the local flame propagation velocity(S_{av}) versus time after ignition for the local area.

4. Conclusion

High-speed images have been acquired for a propagating premixed flame interacting with multiple obstacles in an explosion chamber. The images were processed to obtain the temporally resolved flame-front contours in the area of interest around the obstacle. An in-house FORTRAN code is further developed to determine the local flame propagation velocity. The results showed that overall the flame propagation slows down slightly after impinging onto the obstacle and accelerates again after flame front reconnection. The average of the local flame propagation velocity increases drastically when the flame impinges onto the obstacle. It follows then a decreasing trend and rises again after flame reconnection behind the obstacle wake.

References

1) D. J. Park, A. R. Green, Y. S. Lee, Y. C. Chen, "Experimental studies on interactions between a freely propagating flame and single obstacles in a rectangular confinement", Combustion and Flame, Vol. 150, pp. 27~39, 2007.

2) G. K. Hargrave, S. J. Jarvis and T. C. Williams, "A study of transient flow turbulence generation during flame/wall interactions in explosions", Measurement Science and Technology, Vol. 13, pp. 1036~1042, 2002.

3) I. O. Moen, M. Donato, R. Knystautas, J. H. Lee, "Flame acceleration due to turbulence produced by obstacles", Combustion and Flame, Vol. 39, pp. 21~32, 1980.

4) A. R. Masri, S. S. Ibrahim, N. Nehzat, A. R. Green, "Experimental study of premixed flame propagation over various solid obstructions", Experimental Thermal and Fluid Science, Vol. 21, pp. 109~116, 2000.

5) S. S. Ibrahim, G. K. Hargrave, T. C. Williams, "Experimental investigation of flame/solid interactions in turbulent premixed combustion", Experimental Thermal and Fluid Science, Vol. 24, pp. 99~106, 2001.

6) H. Phylaktou, G. E. Andrews, "Gas explosions in long closed vessels", Combustion Science and Technology, Vol. 77, pp. 27~39, 1991.